International Journal of Pharmaceutics 653 (2024) 123903

Contents lists available at ScienceDirect

International Journal of Pharmaceutics

journal homepage: www.elsevier.com/locate/ijpharm

Surfactants for stabilization of dermal emulsions and their skin compatibility under UVA irradiation: Diacyl phospholipids and polysorbate 80 result in high viability rates of primary human skin cells

Katja Steiner [a], Jakob Josef Schmolz [a], Felisa Hoang [a], Hanna Wolf [a], Saskia Seiser [b], Adelheid Elbe-Bürger [b], Victoria Klang [a,*]

[a] University of Vienna, Department of Pharmaceutical Sciences, Division of Pharmaceutical Technology and Biopharmaceutics, Josef-Holaubek-Platz 2, 1090 Vienna, Austria
[b] Medical University of Vienna, Department of Dermatology, Währinger Gürtel 18-20, 1090 Vienna, Austria

ARTICLE INFO

Keywords:
NRU phototoxicity assay
O/w emulsion
Phospholipids
Primary human dermal fibroblasts
Surfactants
Primary human keratinocytes

ABSTRACT

Phospholipids are versatile formulation compounds with high biocompatibility. However, no data on their effect on skin in combination with UVA radiation exist. Thus, it was the aim of this work to (i) develop o/w nanoemulsions (NEs) differing in surfactant type and to investigate their physicochemical stability at different storage temperatures, (ii) establish a standardized protocol for *in vitro* phototoxicity testing using primary human skin cells and (iii) investigate the phototoxicity of amphoteric phospholipids (S45, S75, E80, S100, LPC80), sodium lauryl ether sulfate (SLES) and polysorbate 80 (PS80). Satisfying systems were developed with all surfactants except S100 due to low zeta potential (-21.4 mV ± 4.69). SLES and PS80-type NEs showed the highest stability after eight weeks; temperature-dependent variations in storage stability were most noticeable for phospholipid surfactants. For phospholipid-based NEs, higher phosphatidylcholine content led to unstable formulations. Phototoxicity assays with primary skin fibroblasts confirmed the lack of UVA-related phototoxicity but revealed cytotoxic effects of LPC80 and SLES, resulting in cell viability as low as 2.7 % ± 0.78 and 1.9 % ± 1.57 compared to the control. Our findings suggest that surfactants S45, S75 and PS80 are the most promising candidates for skin-friendly emulsifiers in sensitive applications involving exposure to UV light.

1. Introduction

Phospholipid-based surfactants are versatile formulation compounds that have been introduced to pharmaceutical product development from the nutrition sector (Ozturk and McClements, 2016; Samdani et al., 2018). Phospholipids are naturally occurring lipids with varying head groups and fatty acid residues. Their common structure is the phosphate group, which – in case of glycerophospholipids – is esterified to a glycerol backbone. Different alcohols, as shown in Fig. 1A, can be esterified to the phosphate group, dividing phospholipids into specific types, e.g., phosphatidylcholine (PC), phosphatidylethanolamine (PE), phosphatidylglycerol (PG), phosphatidylserine (PS) or phosphatidylinositol (PI).

Frequently, the main phospholipid PC is also called lecithin. It is important to note that "lecithin" can encompass various definitions or interpretations, so clarity on its specific context is crucial: while sometimes it is used synonymously with PC, the United States Pharmacopeia describes lecithin as a complex mixture which can contain different phospholipids and other substances such as triglycerides, fatty acids, and carbohydrates. Therefore, it is recommended in the literature to use the term "lecithin" only when the product contains less than 80 % (w/w) phospholipids and the term "phospholipid" when the product contains

Abbreviations: CPZ, chlorpromazine hydrochloride; DMEM, Dulbecco's Modified Eagle's Medium; EtOH, ethanol; FBS, fetal bovine serum; FFA, free fatty acids; GRAS, generally recognized as safe; HLB, hydrophilic-lipophilic balance; KGM-2, Keratinocyte Growth Medium 2; LPC, lyso-phosphatidylcholine; MAPC, monoacyl-phosphatidylcholine; MCT, medium-chain triglycerides; NE, nanoemulsion; NRU, neutral red uptake; PBS, phosphate buffered saline; PC, phosphatidylcholine; PE, phosphatidylethanolamine; PG, phosphatidylglycerol; PI, phosphatidylinositol; PS, phosphatidylserine; PDI, polydispersity index; POE, polyoxyethylene; PS80, polysorbate 80; ROS, reactive oxygen species; SLES, sodium lauryl ether sulfate; ZP, zeta potential.

* Corresponding author.
E-mail address: victoria.klang@univie.ac.at (V. Klang).

https://doi.org/10.1016/j.ijpharm.2024.123903
Received 14 December 2023; Received in revised form 25 January 2024; Accepted 9 February 2024
Available online 11 February 2024

80 % – 100 % (w/w) phospholipids (Drescher and van Hoogevest, 2020).

The glycerol backbone of a phospholipid is esterified with two fatty acids, which can vary in length and degree of saturation. Depending on the natural source from which the phospholipids are derived, they possess different properties. For example, PC derived from egg yolk has a lower content of polyunsaturated fatty acids compared to PC obtained from soybean (van Hoogevest et al., 2011). The main fatty acids of soybean phospholipids are saturated palmitic and polyunsaturated linoleic acid, whereas egg phospholipids mainly contain palmitic and monounsaturated oleic acid (van Hoogevest and Wendel, 2014).

If only one fatty acid is esterified to the glycerol backbone, the molecule is called monoacyl phospholipid or lyso-phospholipid. These phospholipids possess a cone shape and form micelles upon hydration, whereas diacyl phospholipids have a cylindrical shape and form lamellar structures, or, if the polar head groups is small compared to the fatty acid part, possess an inverted cone shape and form inverse micelles (van Hoogevest et al., 2011).

Natural phospholipids can be isolated from different sources, either from vegetables such as soybeans, rape seed, wheat germ and sunflower or from animal material such as egg yolk, milk, or krill. The production from crude vegetable oil includes multiple extraction steps and chromatographic purification procedures, resulting in different fractions with varying PC content (20 % – 98 % w/w). Egg phospholipids are obtained from egg yolk with similar methods. For acyl modification, for example to acquire monoacyl phospholipids, different natural enzymes can be used (van Hoogevest and Wendel, 2014).

While established in parenteral and pulmonal applications (van Hoogevest et al., 2011; Wauthoz and Amighi, 2014), phospholipids are still not standard emulsifiers in dermal products despite decades of research on colloidal systems for dermal use (Yilmaz and Borchert, 2006; Hasanovic et al., 2010; Hoeller et al., 2010; Schwarz et al., 2012; Wolf et al., 2018). Nonetheless, they possess GRAS status and their high biocompatibility regarding epidermal and dermal cells has previously been confirmed (Vater et al., 2019, 2020, 2022). Previous studies have employed variable oil phases, which might have influenced stability and *in vitro* viability data during cytotoxicity tests (Orchard et al., 2019), thereby impeding comparisons between different surfactant types.

Given their generally high biocompatibility, phospholipids emerge as excellent candidates for sensitive applications such as wound healing (Du et al., 2016; Vater et al., 2022) or for skin exposed to photo-induced stress. The lack of photoactive groups could render them highly suitable for the formulation and development of sunscreen products. Surprisingly, no data are available comparing their biocompatibility under photo stress to that of conventional anionic or non-ionic surfactants. Additionally, their storage stability under non-refrigerated conditions should be considered.

Thus, it was the aim of this work to evaluate how various emulsifier types impact the physicochemical stability of fluid o/w nanoemulsions (NEs) at different storage temperatures. Further, we aimed to investigate the influence of these associated surfactants on *in vitro* cell viability under photo stress. For this purpose, we utilized high-pressure homogenization to generate colloidal o/w emulsions in the submicron range, maintaining a consistent oil content (20 % w/w of medium-chain triglycerides, MCT) and surfactant concentration (5 % w/w). Physicochemical stability was monitored over eight weeks at refrigerated storage (8 °C) and room temperature (23 °C). Dynamic light scattering, laser Doppler electrophoresis, pH analysis and rheological measurements were used to evaluate formulation properties.

For phototoxicity testing, a platform adapted after OECD guideline 432 was established in the lab using a solar simulator cube (SOL500 + UVACube 400, Hoenle, Gilching, Germany). A suitable irradiation regime was set up using chlorpromazine hydrochloride (CPZ) as positive control (known phototoxic potential) and sodium dodecyl sulfate (SDS) as negative control (no reported phototoxic behavior). To achieve higher relevance for human physiology, primary human dermal fibroblasts and keratinocytes were used.

2. Materials and methods

2.1. Materials

Phospholipid-based emulsifiers Lipoid® S45, S75, S100, E80 and P-LPC80 (Fig. 1B) were kindly provided by Lipoid GmbH (Ludwigshafen,

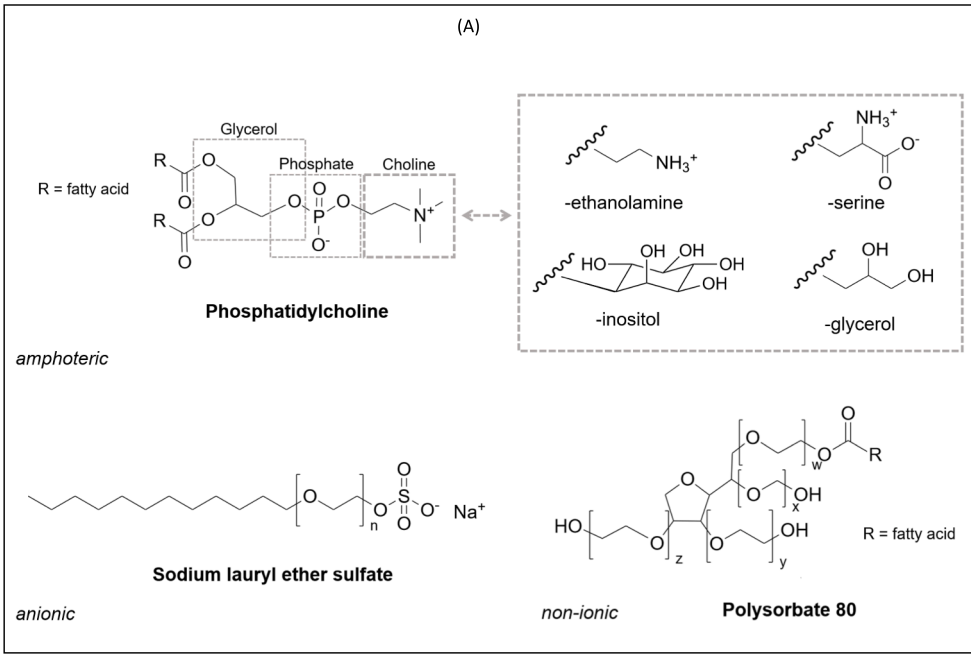

(B)

Composition of NEs	% (w/w)
Medium-chain triglycerides	20
Surfactant	5
Distilled water	75

Codes	Surfactant
NE S45	Lipoid® S45
NE S75	Lipoid® S75
NE S100	Lipoid® S100
NE E80	Lipoid® E80
NE LPC80	Lipoid® PLPC80
NE SLES	Sodium lauryl ether sulfate
NE PS80	Polysorbate 80

(C)

Phospholipid	PC	MAPC	PE
Soybean			
S45	60.2	1.3	15.7
S75	73.6	1.5	9
S100	96.5	1.7	<0,1
PLPC80	5	82	
Egg yolk			
E80	80.3	1.9	7.9

Fig. 1. (A) Chemical structures of investigated surfactants: phospholipids with varying fatty acid residues, SLES (n = 1 – 4), PS80 (w + x + y + z = 20); **(B)** Composition and nomenclature of o/w nanoemulsions; **(C)** Lipid composition of main polar phospholipid constituents and abbreviations: phosphatidylcholine (PC), monoacyl-phosphatidylcholine (MAPC), phosphatidylethanolamine (PE).

GER). Sodium lauryl ether sulfate (SLES) was obtained from Caesar & Loretz GmbH (Hilden, GER). Medium-chain triglycerides (MCT) were purchased from Herba Chemosan (Vienna, AUT). Polysorbate 80 (PS80, Tween®80), neutral red (NR) and chlorpromazine hydrochloride (CPZ) were obtained from Sigma-Aldrich (St. Louis, MO, USA). Dulbecco's Modified Eagle's Medium (DMEM) and fetal bovine serum (FBS) were obtained from Gibco by Life Technologies Limited (Paisley, UK). Penicillin-Streptomycin was obtained from Biowest SAS (Nuaillé, FR). Keratinocyte Growth Medium 2 (KGM-2) was purchased from Bio-medica Medizinprodukte GmbH (Vienna, Austria).

2.2. Preparation of oil-in-water emulsions

Oil-in-water nanoemulsions (NEs) containing 20 % (w/w) MCT and 5 % (w/w) surfactant, comprising either phospholipid-based emulsifiers or conventional surfactants, were developed. Nomenclature and composition of the NEs as well as chemical structures of the investigated surfactants are shown in Fig. 1B and 1C.

For preparation, the respective surfactant was dissolved in water or oil, according to its hydrophilic-lipophilic balance (HLB value), using a magnetic stirrer at 60 °C. The oil phase was slowly added to the aqueous phase under stirring, followed by pre-homogenization with a rotor–-stator device (Ultra-Turrax Omni 5000, Omni International, Kennesaw, GA, USA) for three minutes at 2000 rpm. Afterwards, formulations were treated with a high-pressure homogenizer (Emulsiflex C3, Avestin, Mannheim, Germany) for seven minutes at 700 bar to produce 20.0 g of formulation. After preparation, each formulation was divided into two parts and stored at either 8 °C or 23 °C (n = 3, respectively) to compare the influence of different storage conditions. Initial measurements for characterization were conducted one day after preparation, and stability tests were performed fortnightly over an observation period of eight weeks. Due to the large volume of sample required for rheological assessment, the used NEs were produced separately; rheological measurements were conducted one day after preparation and after eight weeks.

2.3. Dynamic light scattering: Hydrodynamic diameter and polydispersity index

Dynamic light scattering was used to determine hydrodynamic diameter (z-average) and polydispersity index (PDI), using a Zetasizer Nano ZS (Malvern Instruments, Malvern, UK). The dilution range was set at 1:200 (v/v), as previously confirmed to be suitable to avoid multiple scattering of light (Vater et al., 2019). Samples were diluted with freshly distilled water.

2.4. Laser Doppler electrophoresis: Zeta potential

NEs were analysed by laser Doppler electrophoresis to determine zeta potential (ZP), using a Zetasizer Nano ZS (Malvern Instruments, Malvern, UK). Sample dilution of 1:200 (v/v) was done using distilled water, as recently shown to be representative for similar emulsions when compared to diluted saline (Klang et al., 2023).

2.5. pH

pH values of NEs were measured using a Seven Compact pH meter at 23 °C (Mettler Toledo, Columbus, OH, USA).

2.6. Rheological assessment

Dynamic viscosity (η) was analysed at 23 °C in dependence of shear rate at 1 to 100 s^{-1} with a modular compact rheometer (MCR 302 with RheoPlus®Software, Anton Paar GmbH, Graz, Austria). A double-gap measuring system (DG-27, diameter 27 mm) with 8.0 mL sample volume was used for the fluid NEs. Flow curves were established by plotting shear stress (τ) against shear rate ($\dot{\gamma}$). The power law index (n) and flow consistency (k) according to Ostwald-de Waele's power law approach, a widely used simplified model to describe the rheological behavior of Newtonian and non-Newtonian fluids that do not show yield stress property (Ansari et al., 2020), were determined by curve fitting the rheological measurements using the following equation:

$$\tau = k \bullet \dot{\gamma}^n$$

Newtonian fluids show a power law index of 1, while values below 1 imply pseudoplastic flow behavior. Changes in dynamic viscosity after eight weeks were assessed at 10 s^{-1}.

2.7. Thermal stability stress test

To assess the thermal stability of produced NEs, additional stability tests at elevated temperature were performed. NEs were stored at 40 °C over an observation period of eight weeks (n = 3). Hydrodynamic diameter, PDI and pH values were initially analyzed one day after preparation and subsequent measurements were conducted after two, four and eight weeks.

2.8. Cell viability assays

2.8.1. Isolation and culture of primary human skin fibroblasts and keratinocytes

Skin samples from anonymous healthy female and male donors were obtained during plastic surgery procedures from the abdomen, breast or back. The study was approved by the ethics committee of the Medical University of Vienna (ECS 1969/2021) and conducted according to the principles of the Declaration of Helsinki. Written informed consent was obtained from all participants. The isolation was conducted as previously described (Vater et al., 2019). For cultivation, DMEM supplemented with 10 % (v/v) FBS and 1 % (v/v) penicillin–streptomycin (10.000 U/mL) for fibroblasts and serum-free KGM-2 for keratinocytes was used, and cells were cultured at 37 °C and 5 % CO_2. Culture medium was changed every four to six days for fibroblasts and every two to three days for keratinocytes.

2.8.2. NRU phototoxicity assays

The neutral red uptake (NRU) phototoxicity assay, adapted after OECD Guideline 432 (OECD/OCDE., 2019), was established in our lab to screen the investigated surfactants for cytotoxicity and phototoxicity. The NRU phototoxicity assay compares the cytotoxicity of a chemical when tested in presence vs. absence of exposure to simulated solar light. The weakly cationic dye neutral red (NR) penetrates cell membranes at physiological pH and accumulates intracellularly in lysosomes, where it becomes charged and is retained due to the lower pH. If the pH gradient cannot be maintained, e.g., due to formation of reactive oxygen species (ROS) which lead to cell damage and increased permeability of the lysosomal membrane, NR uptake and trapping decreases. Thus, cell viability can be measured (Borenfreund and Puerner, 1985; Repetto et al., 2008; OECD/OCDE., 2019).

Cells were seeded at a density of 7 x 10^3 (fibroblasts) or 1 x 10^4 (keratinocytes) cells per well on 96-well flat-bottom plates (Greiner bio-One, Solingen, Germany) to obtain an approximately half confluent monolayer after 24 h incubation. Two plates per assay were prepared simultaneously. After incubation for 24 h at 37 °C and 5 % CO_2 air atmosphere, the cells were washed with phosphate-buffered saline (PBS) and pre-treated with the respective surfactant. The prepared NEs proved unsuitable to be tested in the NRU phototoxicity assay, as their turbidity (even when diluted) prevented the UVA radiation from reaching the cell layer. Thus, transparent surfactant solutions were prepared to avoid UVA attenuation by the applied samples. According to solubility, the surfactant was either dissolved directly in DMEM or KGM-2 without phenol red or dissolved in ethanol (EtOH) and diluted with phenol red-free DMEM or KGM-2 (1 % v/v EtOH). For the latter, solvent controls

that were treated with culture medium containing 1 % (v/v) EtOH were included.

After incubation with 100 µL surfactant solution for one hour, one plate was irradiated with 1.5 J/cm^2 UVA while the control plate was stored in the dark. To ensure equivalent conditions for both plates, the control plate was wrapped in aluminum foil for light protection and placed in the UVA cube for the same duration as the irradiated plate. Cells were again washed with PBS and the treatment medium was replaced with fresh culture medium, followed by 24 h of incubation.

Cells were washed with PBS before adding 100 µL neutral red medium (50 µg/mL). NR medium was freshly prepared for each test by diluting NR stock solution (5 mg/mL NR in PBS) with pre-warmed culture medium supplemented with 25 mmol/L HEPES to prevent crystallization of NR due to a shift in pH (Baker, 1998; OECD/OCDE., 2019). The stock solution was stored for up to two months (Repetto et al., 2008), protected from light.

After incubation for 3 h, cells were washed with PBS and 150 µL NR desorb solution containing 49 % (v/v) water, 50 % (v/v) EtOH and 1 % (v/v) acetic acid was added. The plates were placed on a microtiter plate shaker for 10 min at 150 rpm, until the NR had formed a homogenous solution. Optical density was measured at 540 nm, using a multiwell plate reader (Tecan^{TM} Infinite 200, Tecan Ltd., Maennedorf, Switzerland). Cell viability in percent was expressed in relation to the viability of control cells, with results presented as means ± standard deviation (SD).

To validate the method for our lab, CPZ as positive control and SDS as negative control were tested and compared to reference values (OECD/OCDE., 2019).

2.8.3. Irradiation setup

For UVA irradiation, a solar simulator (SOL500 + UVACube 400, Hoenle, Gilching, Germany) with H1 filter glass to eliminate UVB radiation was employed. UVA irradiance was measured prior to every use with a UVA meter (UV meter 3.0 with UVA surface sensor, Hoenle, Gilching, Germany). The radiation intensity, as measured through the lid of a 96-well plate, was adjusted by inserting stainless-steel grids between the light source and the irradiated cells. Different mesh sizes were tested to obtain an irradiance of 1.6 – 1.7 mW/cm^2, as recommended by the OECD (OECD/OCDE., 2019). The combination of two grids with 30 and 120 mesh (0.6 mm and 0.125 mm aperture), respectively, was used to achieve the recommended values. Irradiation dose was adjusted by varying the exposure time using the following equation:

$$t\,[\mathrm{min}] = \frac{\text{irradiation dose}\,[\mathrm{J/cm^2}] \times 1000}{\text{irradiance}\,[\mathrm{mW/cm^2}] \times 60}$$

Preliminary studies with different exposure times were performed to investigate the suitable irradiation dose for the employed cell line.

2.8.4. Calculation of PIF and IC_{50}

All surfactants were tested at the highest recommended concentration of 1000 µg/mL. Compounds that do not exhibit any significant cytotoxicity under irradiation up to this limit can be considered as being devoid of relevant phototoxicity. Often, the limit can even be lowered to 100 µg/mL (Ceridono et al., 2012; EMA, 2015).

If cytotoxicity was observed at the limit concentration, the respective surfactant was tested at different concentrations to calculate the respective IC_{50} value and photo irritation factor (PIF) according to the following equation:

$$\mathrm{PIF} = \frac{IC_{50}\,(-\mathrm{UV})}{IC_{50}\,(+\mathrm{UV})}$$

IC_{50} and PIF were calculated using the Phototox 2.0 Software supplied by the OECD. A PIF below 2 implies no phototoxicity for the investigated chemical.

2.9. Statistical analysis

Results are expressed as means ± standard deviation (SD). Data analysis was performed with JASP 0.17.1.0 software using the Student's *t*-test or one-way ANOVA + post-hoc Tukey test with a significance threshold of $p < 0.05$. The Shapiro-Wilk test was used as test of normality. In case of non-parametric data, the *t*-test was replaced by the Wilcoxon signed-rank test (for paired samples) or Mann-Whitney *U* test (for independent samples), and Kruskal-Wallis test + post-hoc Dunn's test was used instead of ANOVA. Outliers in the cell culture data were identified and excluded using the Dixon's Q test with $p < 0.05$.

3. Results and discussion

3.1. Impact of surfactant type on NE properties

Hydrodynamic diameter, polydispersity index and zeta potential.

NEs with hydrodynamic diameter (D_h) between 119 nm and 218 nm were produced (Fig. 2A). Owing to their higher HLB, lower critical packing parameter and higher emulsifying properties, formulations with SLES and PS80 showed the smallest D_h, followed by LPC80. Average size of the diacyl phospholipid based NEs (S45, S75, E80) was comparable, except for NE S100 with larger hydrodynamic diameter. The observed behavior of the phospholipids is in accordance with reported HLB values, with LPC80 possessing the highest (9.1 – 11.3) and S100 the lowest (7.0 – 9.6) HLB range (Otto et al., 2020). The oil phase, MCT, requires an approximate HLB of 11. The HLB of the emulsification system should be close to the required HLB of the oil to obtain good stability and small D_h; when the HLB values are close, the surfactant molecules are arranged more closely on the oil–water interface (Wang et al., 2023). Given that the HLB range of S100 is furthest below the required HLB, it is not surprising that NE S100 exhibited the largest droplet size.

Additionally, the PDI was assessed for all formulations. The PDI describes the degree of non-uniformity of a size distribution (Bera, 2015; Danaei et al., 2018). All NEs showed satisfying homogeneity with PDI values below 0.2 and were therefore suitable for dynamic light scattering measurements (Fig. 2A).

Zeta potential (ZP) was in the negative range for all NEs (Fig. 2B). Values were generally more negative than −40 mV for all NEs, with NE S100 being the only exception. A high absolute ZP above 30 mV is often used as an indicator predicting long-term stability (Bhattacharjee, 2016). The fact that zwitterionic PC, which has a neutral charge at physiological pH, is not contributing to the negative ZP (Klang and Valenta, 2011; Drescher and van Hoogevest, 2020) is apparent due to the significantly lower absolute ZP of NE S100 (consisting almost exclusively of PC) compared to the other formulations ($p < 0.05$). NE SLES showed the most negative ZP, which can be explained by the negative charge of the sulfate head group. Possibly owing to the presence of negatively charged phospholipids at neutral pH, phosphatidylinositol (PI) and phosphatidic acid (PA), NE S45 and NE S75 showed similarly high absolute ZP values (S45: 1.6 % w/w PI and 1.5 % w/w PA, S75: 0.6 % w/w PI and 1.1 % w/w PA, as derived from the certificate of analysis). NE E80, NE LPC80 and NE PS80 exhibited comparable ZP values between −40 and −55 mV (Fig. 2B).

Chemical stability and pH.

pH values of NEs covered a wide range from 4.4 to 7.4, with NE PS80 exhibiting the lowest and NE SLES the highest pH (Fig. 2C). PS80, a heterogenous mixture of polyethoxylated products with polyoxyethylene (POE) sorbitan monooleate as the main component (Zhang et al., 2012; Larson et al., 2020), is susceptible to degradation by oxidation and hydrolysis. Autoxidation, e.g. by temperature and light, occurs mostly on the POE chains, which may lead to formation of POE esters, ketones, aldehydes and acids (Donbrow et al., 1978; Kishore et al., 2011). This, in turn, could lead to a decrease in pH value and is a possible explanation for the observed low pH of NE PS80 (Yi et al., 2020).

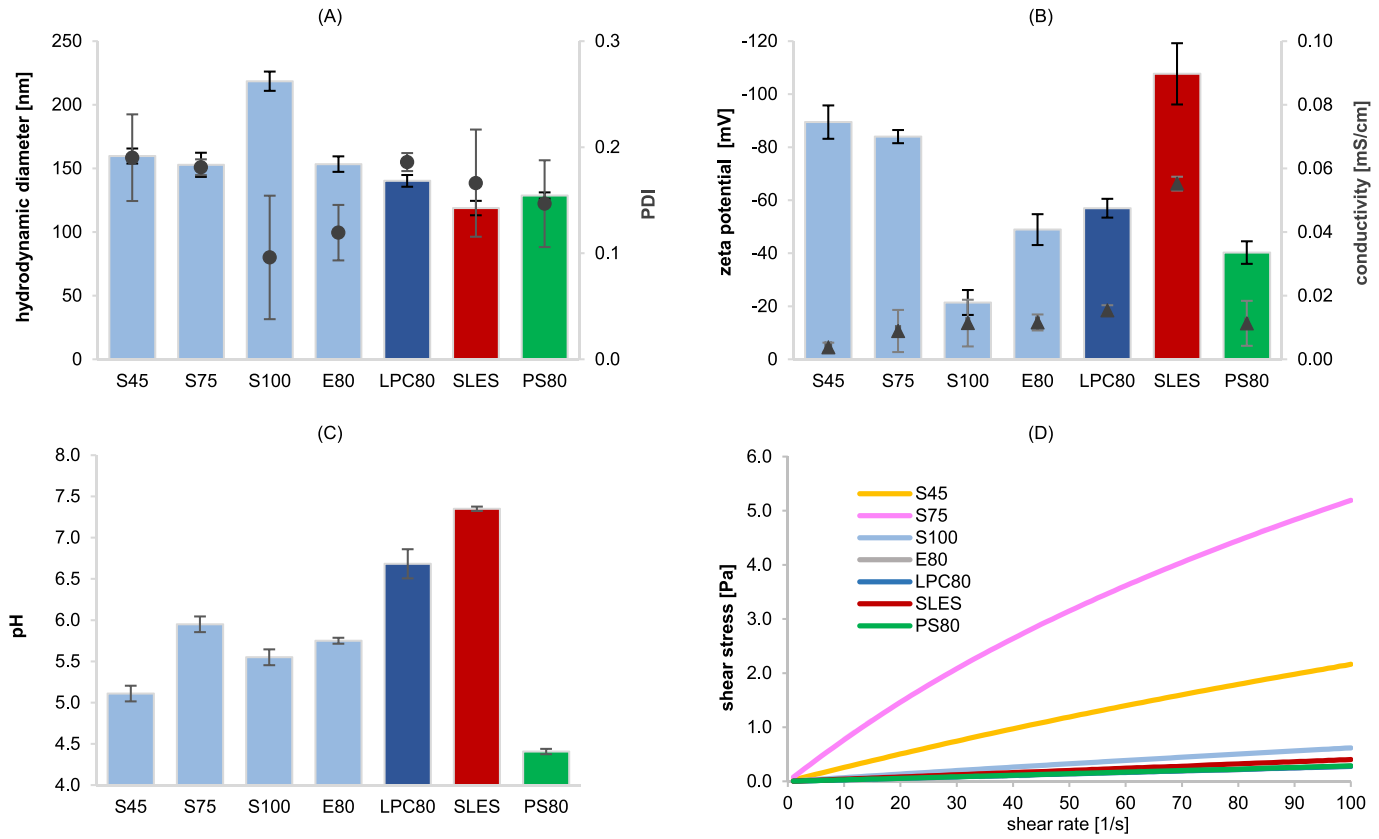

Fig. 2. **(A)** Hydrodynamic diameter (D_h, z-average in nm, left-hand scale, bars) and polydispersity index (PDI, right-hand scale, dots) of o/w nanoemulsions as determined by dynamic light scattering; **(B)** Zeta potential (ZP, left-hand scale, bars) and conductivity (right-hand scale, triangles) of o/w nanoemulsions as determined by laser Doppler electrophoresis; **(C)** pH of o/w nanoemulsions; **(D)** Flow curves of o/w nanoemulsions at a shear rate of 1 to 100 s^{-1}, analysed at 23 °C. For all data (A-D), values are means of n = 3 independent formulations.

The diacyl phospholipid based NEs showed ideal pH for skin care products with values ranging from 5.1 (NE S45) to 6.0 (NE S75) (Wohlrab and Gebert, 2018). The significantly lower pH of NE S45 compared to the other phospholipids ($p < 0.05$) can be explained by its acid value of 16, with corresponding higher amount of free fatty acids (FFA) compared to S75 and E80 with acid values of 8 or S100 with < 0.05 % (w/w) FFA. While the pH of phospholipid-based NEs S75, S100 and E80 was similar, it was significantly higher for NE LPC80 with an average value of 6.7 ($p < 0.05$), which is less desirable regarding skin application.

Rheological profile.

Rheological behavior was dependent on surfactant type and showed remarkable differences between the phospholipids. Flow curves are presented in Fig. 2D. The NEs showed nearly Newtonian flow with a slight tendency to pseudoplastic flow behavior, as can be seen by the corresponding power law indices in Table 1. NE S45 and NE S75 exhibited more pronounced shear thinning as well as considerable higher dynamic viscosity (correlation between applied shear rate and measured shear stress). A slight shear thinning effect was previously observed for fluid NEs (Klang et al., 2011, 2023), possibly due to changes in the droplet shape along the flow channel (Schalbart et al., 2010). An exemplary comparison of dynamic viscosity was conducted at a shear rate of 10 s^{-1} to highlight the differences between NEs: NE LPC80, NE E80, NE SLES and NE PS80 showed viscosity values between 2.8 and 4.0 mPa·s, NE S100 expressed higher viscosity of 6.9 mPa·s (±0.07). Compared to NE S100, NE S45 showed a 3.7-fold increase in viscosity (25.8 mPa·s ± 0.81). S75 acted even more strongly as viscosity enhancer; NE S75 showed dynamic viscosity of 76.7 mPa·s (±3.41), which is an 11-fold increase compared to S100 ($p < 0.05$). A possible explanation for the observed differences in dynamic viscosity might be the largely differing ZP values. NE S45 and NE S75, which showed high absolute ZP, were more viscous than NE S100 with low absolute ZP. Increased absolute ZP in small particles leads to induced repulsion and enhanced thickness of the electrical double layer, which in turn increases viscosity of the emulsion system, particularly at low shear rates (Maranzano and Wagner, 2001; Nakamura et al., 2021). With decreasing absolute ZP, the zero shear viscosity plateau decreases and the shear thinning gradient decreases (Nakamura et al., 2021).

Table 1
Rheological parameters of NEs as calculated using Ostwald-de Waele's power law model. The coefficient of determination, R^2, was above 0.99 for all formulations, indicating accurate fit of the corresponding regression curve.

NE	flow consistency (*k*)	power law index (*n*)
NE S45	0.029	0.94
NE S75	0.101	0.87
NE S100	0.008	0.96
NE E80	0.003	1.00
NE LPC80	0.003	0.99
NE SLES	0.004	0.99
NE PS80	0.003	0.97

3.2. Impact of storage temperature on NE stability

Hydrodynamic diameter, polydispersity index and zeta potential.

Over the eight-week period, the hydrodynamic diameter of most NEs exhibited minimal fluctuations, generally remaining within a 10 % range (Fig. 3A). Overall, storage at 8 °C usually promoted better stability than storage at 23 °C. Of note, NE S100 was the only formulation that showed an increase in droplet size above 10 % when stored under

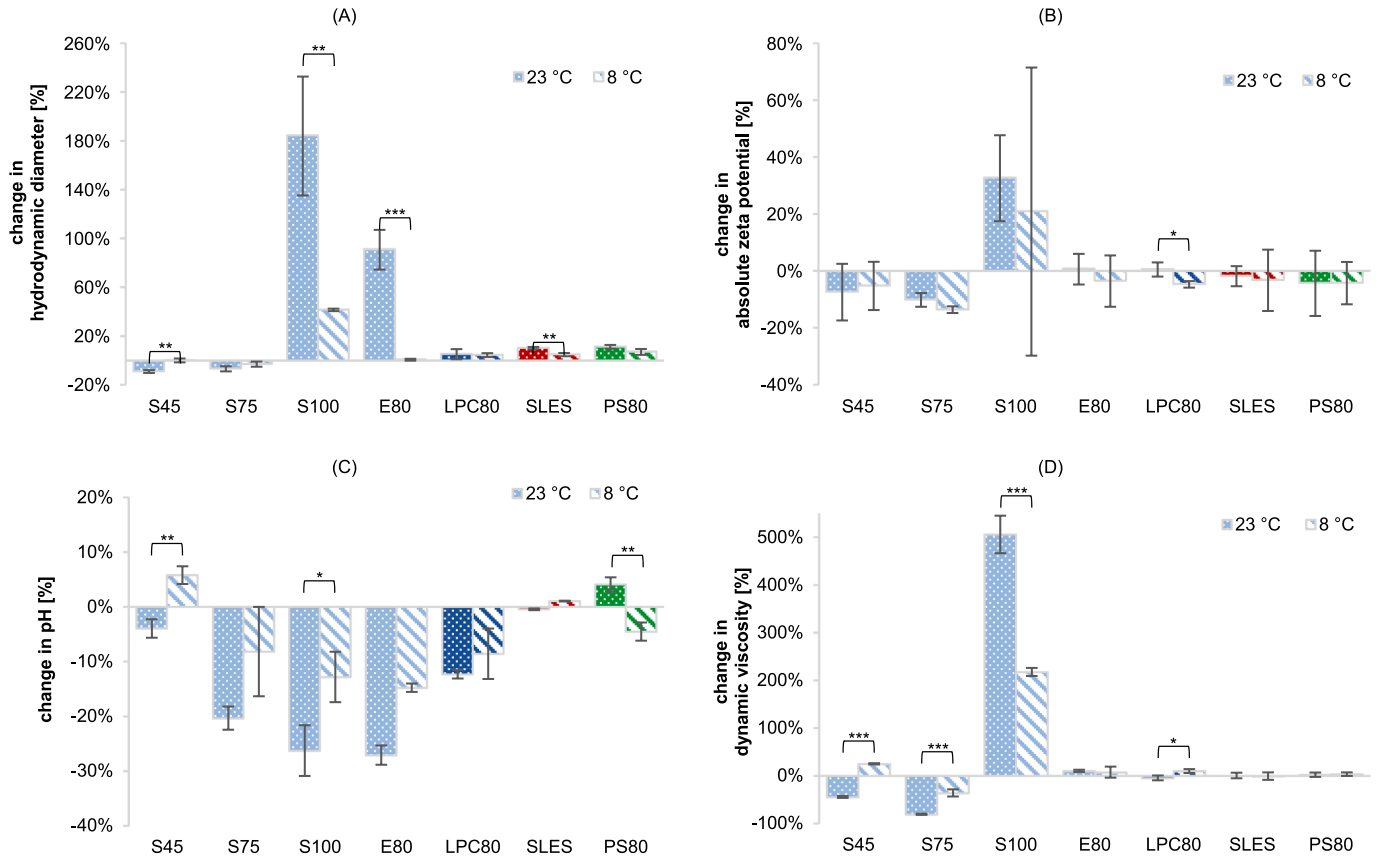

Fig. 3. Change in **(A)** hydrodynamic diameter (z-average), **(B)** absolute zeta potential, **(C)** pH value, **(D)** dynamic viscosity η of o/w nanoemulsions at a shear rate of 10 s^{-1} and 23 °C, all measured after storage for 8 weeks at 23 °C (dotted bars) or 8 °C (striped bars). Values are means ± SD of n = 3 independent formulations. Statistically significant differences are marked with asterisks (*$p < 0.05$, **$p < 0.01$, ***$p < 0.001$).

refrigerated conditions (+42 % ± 1.0). However, for NEs containing S75, LPC80 or PS80, there were no significant differences between storage temperatures. Hence, these NEs prove to be ideal for room temperature storage, a crucial attribute for their application, such as in sunscreen products.

When stored at 23 °C, NE PS80 showed a slight, though not significant increase in droplet size (+11 % ± 1.6). NE E80 and NE S100, however, were evidently not stable with changes of + 91 % (±16.3) and + 185 % (±48.8), respectively. For NE S100, the pronounced change of hydrodynamic diameter at both storage conditions was not surprising, as the absolute ZP of the formulation was low, implying that droplets were not electrically stabilized and flocculation likely to occur. PC alone is not sufficient to stabilize multiphase systems; phospholipid mixtures lead to more stable emulsions, as the different phospholipids can attribute to higher absolute ZP and higher HLB, as discussed above.

ZP remained largely stable with a slight shift to less negative values for some formulations (Fig. 3B). Storage conditions did not impact ZP to a great extent; the different temperatures yielded comparable results. NE S100 experienced a notable shift to more negative values, possibly owing to elevated surface charge of the emulsion droplets due to ester hydrolysis and the release of FFA (Rabinovich-Guilatt et al., 2005). However, the results showed large fluctuations; measurements were possibly hindered due to the occurring aggregation and the corresponding increase in hydrodynamic diameter, underlining again the pronounced instabilities of this formulation.

Chemical stability and pH.

The majority of formulations showed a more noticeable decrease in pH levels when stored at 23 °C (Fig. 3C). The pH of NE SLES remained constant with changes below 1 %. One viewpoint for discussion is that SLES's ether bonds, known for greater chemical stability compared to ester bonds (Yasmann and Sukharev, 2015) were the least impacted by hydrolysis during storage. Consequently, the release of FFA was minimized, preventing a decline in pH. Phospholipids might have exhibited higher susceptibility to hydrolysis, especially when subjected to elevated storage temperatures. As already observed with the changes in hydrodynamic diameter, NE S100 and E80 with the highest PC content were again the least stable formulations with the largest reduction in pH. This can partly be explained by the faster degradation rate of PC compared to PE (Rabinovich-Guilatt et al., 2005) and the corresponding higher amount of released FFA.

Rheological profile.

Changes in dynamic viscosity were assessed at a shear rate of 10 s^{-1} (Fig. 3D). The formulations with phospholipids E80, monoacyl phospholipids LPC80 and conventional surfactants SLES and PS80 remained stable over the observation period of eight weeks. NE S45 and NE S75 demonstrated a tendency to become more fluid, exhibiting more noticeable changes when stored at room temperature. The substantial rise in viscosity of NE S100 (8 °C: + 217 % ± 8.6; 23 °C: + 506 % ± 39.5) aligned well with the previously discussed instabilities, notably flocculation (Starov and Zhdanov, 2003), further emphasizing the susceptibility of this formulation to destabilization.

3.3. Stability of NEs at elevated temperature

Thermal stability tests were conducted to further investigate the suitability of the used surfactants for sunscreen formulations, considering that these products are expected to be exposed to elevated temperatures. Storage at 40 °C for eight weeks led to noticeable olfactory changes, possibly attributed to oxidative degradation (Genot et al., 2003), for all NEs and pronounced phase separation for NE S100 and

E80, hindering optical and pH analysis. Thus, measurements taken after a storage period of four weeks were used for comparison between NEs (Fig. 4). Change in hydrodynamic diameter showed the same trend as discussed above for storage at lower temperatures: after four weeks, NE S100 and E80 exhibited an increase in droplet size (41 % ± 20.7 and 44 % ± 4.3, respectively), while the other NEs showed minimal fluctuations below 10 %. pH decreased for all NEs except for NE S75, although the high SD of this formulation suggests inconsistencies. Overall, the results of the thermal stability study reflected similar trends as the stability tests at 8 °C and 23 °C with NE S100 and E80 emerging as the least stable formulations.

3.4. Impact of surfactant type and UVA radiation on cell viability

In determining an appropriate radiation regime for primary human skin fibroblasts, we initially explored various irradiation doses aiming to maintain high cell viability (>80 % compared to control cells) while also triggering chemical excitation to elicit a phototoxic reaction. The irradiation dose was modified by altering the duration of exposure time. Irradiation with 1.5 J/cm^2 (15 min 38 sec at 1.6 mW/cm^2) yielded viability rates of 87 % (±19.3, n = 5) and induced phototoxic reactions of the positive control (CPZ), but not the negative control (SDS). Therefore, 1.5 J/cm^2 was selected as suitable irradiation dose and used for all further experiments. IC_{50} and PIF of CPZ and SDS are shown in Table 2. A PIF below 2 implies that the investigated chemical is not phototoxic.

Treatment of fibroblasts with diacyl phospholipids S45, S75, S100 and E80 resulted in consistently high viability rates (85 % – 116 %), both in the presence and absence of UVA irradiation, showing no notable differences among the various phospholipid types (Fig. 5A). PS80 was also well-tolerated, resulting in a cell viability of 85 % (±15.0) for the control plate and 93 % (±3.9) for the irradiated cells. The documented high biocompatibility of PS80 aligns with findings in the literature (Lémery et al., 2015; Ueda et al., 2019; Liu and Lunter, 2020). IC_{50} values were not determined for these surfactants, as the maximum assay concentration of 1000 µg/mL did not substantially affect viability, even under exposure to UVA light. Thus, the diacyl phospholipids and PS80 are considered devoid of any relevant phototoxicity (OECD/OCDE., 2019). The high biocompatibility of phospholipids is consistent with findings in the literature (Weyenberg et al., 2007; Vater et al., 2019, 2020), proving robust even under UVA-induced stress.

LPC80 and SLES were cytotoxic at the limit concentration of 1000 µg/mL, resulting in notably low viability rates (<3%). Hence, lower concentrations of both surfactants were tested to establish their IC_{50} values and calculate PIF. The anionic surfactants SDS and SLES as well as monoacyl phospholipid LPC80 showed comparable IC_{50} and PIF, as shown in Table 2A. While all three surfactants demonstrated cytotoxicity, there was no induction of phototoxicity, indicated by their PIF below 2. The well-established potential for skin irritation, especially for SDS, but also SLES, is documented in literature (Lémery et al., 2015; Mijaljica et al., 2022; Adu et al., 2023). Nonetheless, it was unexpected to note that LPC80 exhibited similar cytotoxicity. Toxicity of surfactants can partly be explained by their interaction with cellular lipid bilayers, resulting in a disruption of the plasma membrane (Maupas et al., 2011). A possible explanation for the vastly differing results between monoacyl phospholipids and diacyl phospholipids might be the higher aqueous solubility and the lower packing parameter of LPC80 compared to the diacyl phospholipids. LPC80 is cone-shaped, forms micelles upon dispersion in water and possesses higher emulsifying properties for stabilization of o/w emulsions or to solubilize lipophilic substances (Hoppel et al., 2014; van Hoogevest and Fahr, 2019), which could negatively impact cell viability.

To further investigate the skin compatibility of the used surfactants in combination with UVA radiation, we additionally conducted the assay using primary human skin keratinocytes. The same irradiation dose as for the fibroblasts proved to be suitable, facilitating comparison between the two cell lines. Results showed the same trends as for the fibroblasts: the diacyl phospholipids and PS80 were tolerated well, while LPC80 and SLES were highly cytotoxic at the limit concentration (Fig. 5B). However, IC_{50} values revealed that keratinocytes were in general more sensitive to the surfactants' toxicity compared to fibroblasts; IC_{50} values of SDS and SLES were about five to six times lower (Table 2B). These findings align with previous results in our research group, where cell viability of keratinocytes after exposure to selected NEs without irradiation was generally lower than viability of fibroblasts (Vater et al., 2019). Of note, compared to SDS and SLES, LPC80 was tolerated better

Table 2
IC_{50} values in µg/mL and PIF of positive and negative control and cytotoxic surfactants (LPC80, SLES). Values are means ± SD of n = 4 tests with 6 parallel experiments.

(A) Primary human skin fibroblasts			
Test chemical	**IC_{50} -UV**	**IC_{50} + UV**	**PIF**
CPZ (positive control)	17.2 (±3.8)	1.9 (±0.4)	9.3 (±2.2)
SDS (negative control)	104.3 (±19.3)	106.0 (±11.0)	1.0 (±0.3)
LPC80	101.9 (±22.6)	87.1 (±27.5)	1.2 (±0.1)
SLES	81.6 (±25.1)	80.3 (±35.6)	1.1 (±0.4)
(B) Primary human skin keratinocytes			
Test chemical	**IC_{50} -UV**	**IC_{50} + UV**	**PIF**
CPZ (positive control)	25.7 (±5.5)	1.9 (±0.3)	13.9 (±4.8)
SDS (negative control)	15.9 (±1.0)	14.9 (±2.3)	1.1 (±0.2)
LPC80	46.7 (±5.3)	38.6 (±5.7)	1.2 (±0.3)
SLES	17.1 (±3.5)	16.4 (±1.8)	1.0 (±0.2)

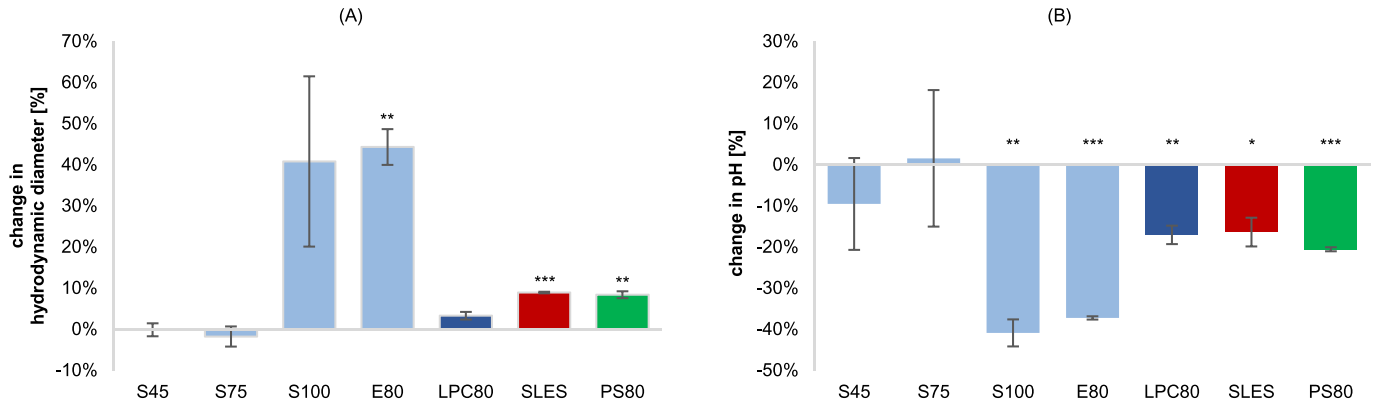

Fig. 4. Change in **(A)** hydrodynamic diameter (z-average) and **(B)** pH value of o/w nanoemulsions after storage for 4 weeks at 40 °C. Values are means ± SD of n = 3 independent formulations. Statistically significant changes between values recorded at week 0 and week 4 are marked with asterisks (*$p < 0.05$, **$p < 0.01$, ***$p < 0.001$).

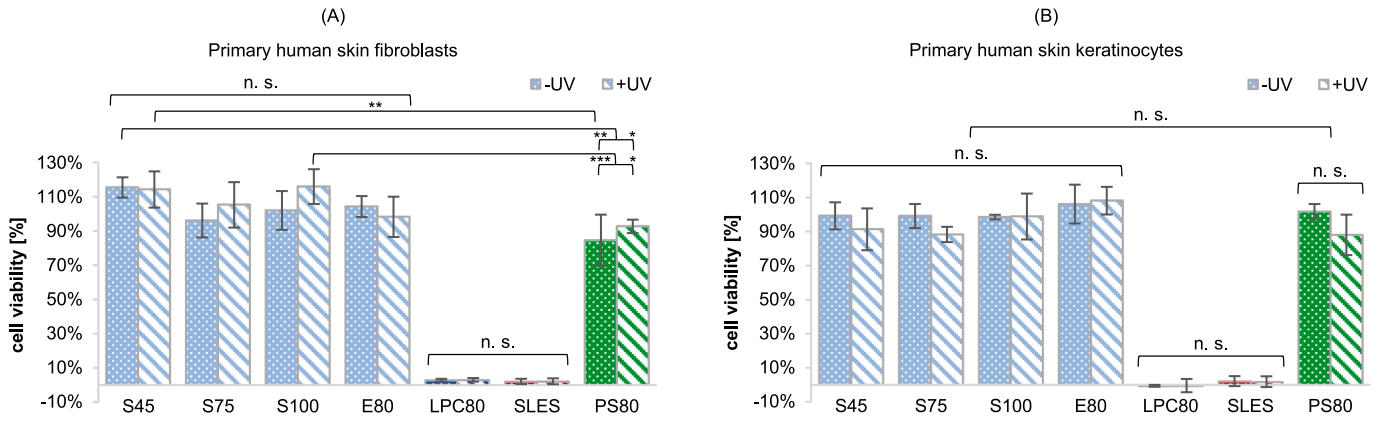

Fig. 5. Cell viability of **(A)** fibroblasts and **(B)** keratinocytes in percent after incubation with the respective surfactant at a concentration of 1000 µg/mL, protected from light (dotted bars) or exposed to 1.5 J/cm^2 UVA radiation (striped bars). Values are means ± SD of n = 5 tests with 6 or 12 parallel experiments. Statistically significant differences between non-cytotoxic surfactants are marked with asterisks (*$p < 0.05$, **$p < 0.01$, ***$p < 0.001$; n. s. = not significant).

by the keratinocytes, with the respective IC_{50} being approximately three times higher than the IC_{50} of SDS and SLES (Table 2B).

Our results validated the hypothesis that phospholipids, devoid of photoactive groups, would not elicit any phototoxic reactions. Even when exposed to UVA radiation, they demonstrate high skin compatibility, much like PS80. As anticipated, SDS and SLES displayed high cytotoxicity without exhibiting any phototoxic potential. Surprisingly, the same magnitude of cytotoxicity was observed for LPC80 in case of fibroblasts, and to a lesser extent for keratinocytes.

Further *ex vivo* and *in vivo* studies are planned to verify biocompatibility of phospholipids in combination with UVA radiation.

4. Conclusion

Of the tested phospholipid-based surfactants, S45, S75 and LPC80 exhibited highest potential for stabilization of submicron-sized o/w emulsions also when subjected to thermal stress (40 °C over four weeks without preserving agents, antioxidants, or stabilizers), suggesting similar potential for stabilization of sunscreen products as SLES and PS80. All tested surfactants (amphoteric phospholipids, anionic SLES, non-ionic PS80) were devoid of UVA-related phototoxicity in NRU assays. However, both SLES and LPC80 demonstrated cytotoxicity levels comparable to the known irritant SDS for fibroblasts and to a lesser extent for keratinocytes. We conclude that phospholipids S45 and S75 as well as PS80 stand out as the most skin-friendly surfactants for stabilizing sunscreen products.

Financing

The presented work was financed by the Phospholipid Research Center Heidelberg (VKL-2022–099/1–1) and by the Austrian Science Fund (FWF; P31485-B30 and DK W1248-B30 both to AEB) .

CRediT authorship contribution statement

Katja Steiner: Writing – original draft, Validation, Supervision, Methodology, Investigation, Formal analysis, Data curation, Conceptualization. **Jakob Josef Schmolz:** Investigation. **Felisa Hoang:** Investigation. **Hanna Wolf:** Investigation. **Saskia Seiser:** Methodology, Investigation. **Adelheid Elbe-Bürger:** Writing – review & editing, Supervision, Resources, Methodology, Funding acquisition. **Victoria Klang:** Writing – review & editing, Supervision, Resources, Project administration, Methodology, Funding acquisition, Conceptualization.

Declaration of competing interest

The authors declare the following financial interests/personal relationships which may be considered as potential competing interests: [Victoria Klang reports financial support was provided by Phospholipid Research Center. Adelheid Elbe-Buerger reports financial support was provided by Austrian Science Fund. If there are other authors, they declare that they have no known competing financial interests or personal relationships that could have appeared to influence the work reported in this paper].

Data availability

Data will be made available on request.

Acknowledgements

The authors express gratitude to Lipoid GmbH (Ludwigshafen, Germany) for providing surfactants and Jan Steiner for contributing expertise in statistical analysis.

References

Adu, S.A., Twigg, M.S., Naughton, P.J., Marchant, R., Banat, I.M., 2023. Characterisation of cytotoxicity and immunomodulatory effects of glycolipid biosurfactants on human keratinocytes. Appl. Microbiol. Biotechnol. 107, 137–152. https://doi.org/10.1007/s00253-022-12302-5.

Ansari, S., Rashid, M.A.I., Waghmare, P.R., Nobes, D.S., 2020. Measurement of the flow behavior index of Newtonian and shear-thinning fluids via analysis of the flow velocity characteristics in a mini-channel. SN Applied Sci. 2, 1787. https://doi.org/10.1007/s42452-020-03561-w.

Baker, C.S., 1998. Crystallization of neutral red vital stain from minimum essential medium due to pH instability. In Vitro Cell. Dev. Biol. Anim. 34 (8), 607–608. https://doi.org/10.1007/s11626-996-0003-0.

Bera, B., 2015. Nanoporous silicon prepared by vapour phase strain etch and sacrificial technique. Int. Conference on Microelectronic Circuit and System (micro). 42–45.

Bhattacharjee, S., 2016. DLS and zeta potential - What they are and what they are not? J. Control. Release. 235, 337–351. https://doi.org/10.1016/j.jconrel.2016.06.017.

Borenfreund, E., Puerner, J.A., 1985. A simple quantitative procedure using monolayer cultures for cytotoxicity assays (HTD/NR-90). J. Tissue Cult. Methods. 9, 7–9. https://doi.org/10.1007/BF01666038.

Ceridono, M., Tellner, P., Bauer, D., Barroso, J., Alépée, N., Corvi, R., De Smedt, A., Fellows, M.D., Gibbs, N.K., Heisler, E., Jacobs, A., Jirova, D., Jones, D., Kandárová, H., Kasper, P., Akunda, J.K., Krul, C., Learn, D., Liebsch, M., Lynch, A.M., Muster, W., Nakamura, K., Nash, J.F., Pfannenbecker, U., Phillips, G., Robles, C., Rogiers, V., van de Water, F., Wändel Liminga, U., Vohr, H.W., Wattrelos, O., Woods, J., Zuang V., Kreysa, J., Wilcox, P. (2012) The 3T3 neutral red uptake phototoxicity test: Practical experience and implications for phototoxicity testing – The report of an ECVAM–EFPIA workshop. https://doi.org/10.1016/j.yrtph.2012.06.001.

Danaei, M., Dehghankhold, M., Ataei, S., Davarani, F.H., Javanmard, R., Dokhani, A., Khorasani, S., Id, M.R.M., 2018. Impact of particle size and polydispersity index on the clinical applications of lipidic nanocarrier systems. Pharmaceutics. 10 (2), 57. https://doi.org/10.3390/pharmaceutics10020057.

Donbrow, M., Hamburger, R., Azaz, E., Pillersdorf, A., 1978. Development of acidity in non-ionic surfactants: formic and acetic acid. Analyst. 103 (1225), 400–403. https://doi.org/10.1039/AN9780300400.

Drescher, S., van Hoogevest, P., 2020. The phospholipid research center: current research in phospholipids and their use in drug delivery. Pharmaceutics. 12, 1235–1261. https://doi.org/10.3390/pharmaceutics12121235.

Du, L., Feng, X., Xiang, X., Jin, Y., 2016. Wound healing effect of an in situ forming hydrogel loading curcumin-phospholipid complex. Curr. Drug Deliv. 13 (1), 76–82. https://doi.org/10.2174/1567201813666151202195437.
EMA ICH Guidance S10 on Photosafety Evaluation of Pharmaceuticals 2015 European Medicines Agency Committee for Human Medicinal Products.
Genot, C., Meynier, A., Riaublanc, A., 2003. Lipid Oxidation in Emulsions. In: Kamal-Eldin, A. (Ed.), Lipid Oxidation Pathways. AOCS press, Illinois. https://doi.org/10.1201/9781439822098.ch7.
Hasanovic, A., Hollick, C., Fischinger, K., Valenta, C., 2010. Improvement in physicochemical parameters of DPPC liposomes and increase in skin permeation of aciclovir and minoxidil by the addition of cationic polymers. Eur. J. Pharm. Biopharm. 75 (2), 148–153. https://doi.org/10.1016/j.ejpb.2010.03.014.
Hoeller, S., Klang, V., Valenta, C., 2010. Skin-compatible lecithin drug delivery systems for fluconazole: effect of phosphatidylethanolamine and oleic acid on skin permeation. J. Pharm. Pharmacol. 60 (5), 587–591. https://doi.org/10.1211/jpp.60.5.0003.
Hoppel, M., Ettl, H., Holper, E., Valenta, C., 2014. Influence of the composition of monoacyl phosphatidylcholine based microemulsions on the dermal delivery of flufenamic acid. Int. J. Pharm. 475, 156–162. https://doi.org/10.1016/j.ijpharm.2014.08.058.
Kishore, R.S.K., Pappenberger, A., Dauphin, I.B., Ross, A., Buergi, B., Staempfli, A., Mahler, H.C., 2011. Degradation of polysorbates 20 and 80: studies on thermal autoxidation and hydrolysis. J. Pharm. Sci. 100 (2), 721–731. https://doi.org/10.1002/jps.22290.
Klang, V., Valenta, C., 2011. Lecithin-based nanoemulsions. J. Drug Delivery Sci. Technol. 21 (1), 55–76. https://doi.org/10.1016/S1773-2247(11)50006-1.
Klang, V., Schwarz, J.C., Matsko, N., Rezvani, E., El-Hagin, N., Wirth, M., Valenta, C., 2011. Semi-solid sucrose stearate-based emulsions as dermal drug delivery systems. Pharmaceutics. 3, 275–306. https://doi.org/10.3390/pharmaceutics3020275.
Klang, V., Schweiger, E.M., Strohmaier, S., Walter, V.I., Dekic, Z., Tahir, A., 2023. Dermal delivery of korean red ginseng extract: impact on storage stability of different carrier systems and evaluation of Rg1 and Rb1 skin permeation Ex Vivo. Pharmaceutics. 15 (1), 56. https://doi.org/10.3390/PHARMACEUTICS15010056/S1.
Larson, N.R., Wei, Y., Prajapati, I., Chakraborty, A., Peters, B., Kalonia, C., Hudak, S., Choudhary, S., Esfandiary, R., Dhar, P., Schöneich, C., Middaugh, C.R., 2020. Comparison of polysorbate 80 hydrolysis and oxidation on the aggregation of a monoclonal antibody. J. Pharm. Sci. 109, 633–639. https://doi.org/10.1016/j.xphs.2019.10.069.
Lémery, E., Briançon, S., Chevalier, Y., Bordes, C., Oddos, T., Gohier, A., Bolzinger, M.A., 2015. Skin toxicity of surfactants: Structure/toxicity relationships. Colloids and Surfaces A: Physicochemical and Eng. Aspects. 469, 166–179. https://doi.org/10.1016/j.colsurfa.2015.01.019.
Liu, Y., Lunter, D.J., 2020. Systematic investigation of the effect of non-ionic emulsifiers on skin by confocal raman spectroscopy—a comprehensive lipid analysis. Pharmaceutics. 12 (3), 223. https://doi.org/10.3390/pharmaceutics12030223.
Maranzano, B.J., Wagner, N.J., 2001. The effects of interparticle interactions and particle size on reversible shear thickening: Hard-sphere colloidal dispersions. J. Rheol. 45 (5), 1205–1222. https://doi.org/10.1122/1.1392295.
Maupas, C., Moulari, B., Béduneau, A., Lamprecht, A., Pellequer, Y., 2011. Surfactant dependent toxicity of lipid nanocapsules in HaCaT cells. Int. J. Pharm. 411, 136–141. https://doi.org/10.1016/j.ijpharm.2011.03.056.
Mijaljica, D., Spada, F., Harrison, I.P., 2022. Skin cleansing without or with compromise: soaps and syndets. Molecules. 27 (6), 2010. https://doi.org/10.3390/molecules27062010.
Nakamura, H., Makino, S., Ishii, M., 2021. Effects of electrostatic interaction on rheological behavior and microstructure of concentrated colloidal suspensions. Colloids Surf A Physicochem Eng Asp. 623, 126576 https://doi.org/10.1016/j.colsurfa.2021.126576.
Oecd, ocde, Test No. 432. In Vitro 3T3 NRU Phototoxicity Test OECD Guidelines for the Testing Chemicals [preprint] 2019.
Orchard, A., Kamatou, G., Viljoen, A.M., Patel, N., Mawela, P., Vuuren, S.F.V., 2019. The influence of carrier oils on the antimicrobial activity and cytotoxicity of essential oils. Evid. Based Complement. Alternat. Med. 2019, 6981305. https://doi.org/10.1155/2019/6981305.
Otto, F., van Hoogevest, P., Syrowatka, F., Heinl, V., Neubert, R.H.H., 2020. Assessment of the applicability of HLB values for natural phospholipid emulsifiers for preparation of stable emulsions. Pharmazie. 75, 365–370. https://doi.org/10.1691/PH.2020.9174.
Ozturk, B., McClements, D.J., 2016. Progress in natural emulsifiers for utilization in food emulsions. Curr. Opin. Food Sci. 7, 1–6. https://doi.org/10.1016/j.cofs.2015.07.008.
Rabinovich-Guilatt, L., Dubernet, C., Gaudin, K., Lambert, G., Couvreur, P., Chaminade, P., 2005. Phospholipid hydrolysis in a pharmaceutical emulsion assessed by physicochemical parameters and a new analytical method. Eur. J. Pharm. Biopharm. 61, 69–79. https://doi.org/10.1016/j.ejpb.2005.03.001.
Repetto, G., del Peso, A., Zurita, J.L., 2008. Neutral red uptake assay for the estimation of cell viability/cytotoxicity. Nat. Protoc. 3 (7), 1125–1131. https://doi.org/10.1038/nprot.2008.75.
Samdani, G.K., McClements, D.J., Decker, E.A., 2018. Impact of phospholipids and tocopherols on the oxidative stability of soybean oil-in-water emulsions. J. Agric. Food Chem. 66 (15), 3939–3948. https://doi.org/10.1021/acs.jafc.8b00677.
Schalbart, P., Kawaji, M., Fumoto, K., 2010. Formation of tetradecane nanoemulsion by low-energy emulsification methods. Int. J. Refrig. 33, 1612–1624. https://doi.org/10.1016/j.ijrefrig.2010.09.002.
Schwarz, J.C., Klang, V., Hoppel, M., Mahrhauser, D., Valenta, C., 2012. Natural microemulsions: formulation design and skin interaction. Eur. J. Pharm. Biopharm. 81 (3), 557–562. https://doi.org/10.1016/j.ejpb.2012.04.003.
Starov, V.M., Zhdanov, V.G., 2003. Viscosity of emulsions: influence of flocculation. J. Colloid Interface Sci. 258 (2), 404–414. https://doi.org/10.1016/S0021-9797(02)00149-2.
Ueda, Y., Mashima, K., Miyazaki, M., Hara, S., Takata, T., Kamimura, H., Takagi, S., Jimi, S., 2019. Inhibitory effects of polysorbate 80 on MRSA biofilm formed on different substrates including dermal tissue. Sci. Rep. 9 https://doi.org/10.1038/s41598-019-39997-3.
van Hoogevest, P., Fahr, A., 2019. Phospholipids in Cosmetic Carriers. In: Cornier, J., Keck, C., van de Voorde, M. (Eds.), Nanocosmetics. Springer, Cham, pp. 95–140. https://doi.org/10.1007/978-3-030-16573-4_6.
van Hoogevest, P., Wendel, A., 2014. The use of natural and synthetic phospholipids as pharmaceutical excipients. Eur. J. Lipid Sci. Technol. 116 (9), 1088–1107. https://doi.org/10.1002/ejlt.201400219.
van Hoogevest, P., Liu, X., Fahr, A., Leigh, M.L.S., 2011. Role of phospholipids in the oral and parenteral delivery of poorly water soluble drugs. J. Drug Delivery Sci. Technol. 21 (1), 5–16. https://doi.org/10.1016/S1773-2247(11)50001-2.
Vater, C., Adamovic, A., Ruttensteiner, L., Steiner, K., Pooja, T., Klang, V., Adelheid, E.-B., Michael, W., Claudia, V., 2019. Cytotoxicity of lecithin-based nanoemulsions on human skin cells and ex vivo skin permeation: comparison to conventional surfactant types. Int. J. Pharm. 20 (566), 383–390. https://doi.org/10.1016/j.ijpharm.2019.05.078.
Vater, C., Hlawaty, V., Werdenits, P., Cichoń, M.A., Klang, V., Elbe-Bürger, A., Wirth, M., Valenta, C., 2020. Effects of lecithin-based nanoemulsions on skin: Short-time cytotoxicity MTT and BrdU studies, skin penetration of surfactants and additives and the delivery of curcumin. Int. J. Pharm. 580, 119–209. https://doi.org/10.1016/j.ijpharm.2020.119209.
Vater, C., Bosch, L., Mitter, A., Göls, T., Seiser, S., Heiss, E., Elbe-Bürger, A., Wirth, M., Valenta, C., Klang, V., 2022. Lecithin-based nanoemulsions of traditional herbal wound healing agents and their effect on human skin cells. Eur. J. Pharm. Biopharm. 170, 1–9. https://doi.org/10.1016/j.ejpb.2021.11.004.
Wang, Q., Zhang, H., Han, Y., Cui, Y., Han, X., 2023. Study on the relationships between the oil HLB value and emulsion stabilization. RSC Adv. 13, 24692. https://doi.org/10.1039/d3ra04592g.
Wauthoz, N., Amighi, K., 2014. Phospholipids in pulmonary drug delivery. Eur. J. Lipid Sci. Technol. 116 (9), 1114–1128. https://doi.org/10.1002/ejlt.201300368.
Weyenberg, W., Filev, P., Van den Plas, D., Vandervoort, J., De Smet, K., Sollie, P., Ludwig, A., 2007. Cytotoxicity of submicron emulsions and solid lipid nanoparticles for dermal application. Int. J. Pharm. 337, 291–298. https://doi.org/10.1016/j.ijpharm.2006.12.045.
Wohlrab, J., Gebert, A., 2018. PH and buffer capacity of topical formulations. Curr. Probl. Dermatol. 54, 123–131. https://doi.org/10.1159/000489526.
Wolf, M., Klang, V., Stojcic, T., Fuchs, C., Wolzt, M., Valenta, C., 2018. NLC versus nanoemulsions: effect on physiological skin parameters during regular in vivo application and impact on drug penetration. Int. J. Pharm. 549 (1–2), 343–351. https://doi.org/10.1016/j.ijpharm.2018.08.007.
Yasmann, A., Sukharev, S., 2015. Properties of diphytanoyl phospholipids at the air−water interface. Langmuir. 31, 350–357. https://doi.org/10.1021/la503800g.
Yi, Y., Jin, Y., Menon, R., Yeung, B., 2020. Polysorbate, the good, the bad and the ugly. American Pharmaceutical Review - the Review of American Pharmaceutical Business & Technol.
Yilmaz, E., Borchert, H.H., 2006. Effect of lipid-containing, positively charged nanoemulsions on skin hydration, elasticity and erythema - An in vivo study. Int. J. Pharm. 307 (2), 232–238. https://doi.org/10.1016/j.ijpharm.2005.10.002.
Zhang, R., Wang, Y., Tan, L., Zhang, H.Y., Yang, M., 2012. Analysis of polysorbate 80 and its related compounds by RP-HPLC with ELSD and MS detection. J. Chromatogr. Sci. 50 (7), 598–607. https://doi.org/10.1093/chromsci/bms035.